NANO LETTERS

Letter

pubs.acs.org/NanoLett

Metal-Core/Semiconductor-Shell Nanocones for Broadband Solar Absorption Enhancement

Lin Zhou,[†,‡] Xiaoqiang Yu,[§] and Jia Zhu*[,†]

[†]College of Engineering and Applied Sciences, Nanjing University, Nanjing 210093, People's Republic of China

[‡]School of Physics and Electronic Engineering, Nanjing Xiaozhuang University, Nanjing 211171, People's Republic of China

[§]Department of Physics, Southeast University, Nanjing 211189, People's Republic of China

ABSTRACT: Nanostructure-based photovoltaic devices have exhibited several advantages, such as reduced reflection, extraordinary light trapping, and so forth. In particular, semiconductor nanostructures provide optical modes that have strong dependence on the size and geometry. Metallic nanostructures also attract a lot of attention because of the appealing plasmonic effect on the near-field enhancement. In this study, we propose a novel design, the metal-core/semiconductor-shell nanocones with the core radius varying in a linearly gradient style. With a thin layer of semiconductor absorber coated on a metallic cone, such a design can lead to significant and broadband absorption enhancement across the entire visible and near-infrared solar spectrum. As an example of demonstration, a layer of 16 nm thick crystalline silicon (c-Si) coated on a silver nanocone can absorb 27% of standard solar radiation across a broad spectral range of 300−1100 nm, which is equivalent to a 700 nm thick flat c-Si film. Therefore, the absorption enhancement factor approaching the Yablonovitch limit is achieved with this design. The significant absorption enhancement can be ascribed to three types of optical modes, that is, Fabry−Perot modes, plasmonic modes, and hybrid modes that combine the features of the previous two. In addition, the unique nanocone geometry enables the linearly gradient radius of the semiconductor shell, which can support multiple optical resonances, critical for the broadband absorption. Our design may find general usage as elements for the low cost, high efficiency solar conversion and water-splitting devices.

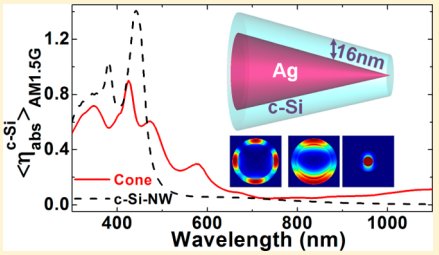

KEYWORDS: *Solar cell, Si, core−shell, nanocone, broadband absorption, plasmonic*

Photon management is critical to photovoltaic (PV) devices. For example, for crystalline silicon (c-Si) solar cells, the dominant player in the PV market, one of the primary tasks is to dramatically reduce the required silicon quantity and quality for the large-scale commercial implementations.[1−3] On the basis of the concept of advanced photon management, a variety of nanostructured PV devices, such as nanowire, nanopillar, nanocone, pyramid, and various other conformal geometries,[4−10] have been explored. However, so far simple and feasible designs with dramatic absorption enhancement factor approaching and beyond the Yablonovitch limit ($4n^2$ limit)[11] have rarely been achieved.

Both semiconductor and metallic nanostructures have been heavily investigated for absorption enhancement effect.[12−18] For example, by employing semiconductor nanowires or nanoshells with radius dispersed in a certain extent,[13,14] more optical modes are involved, which can result in the broadband light absorption. The other promising pathway for absorption enhancement is to employ the plasmonic effect of metallic nanostructures.[15−18] For example, by introducing metallic nanoparticles or periodically arranged metallic structures, the electromagnetic (EM) field can be greatly enhanced in close proximity to the metallic surface due to the localized surface plasmon (LSP) or surface plasmon polariton excitations.[19,20] However, very few designs combining both of two mechanisms have been explored so far.

In this work, a design of metal-core/semiconductor-shell nanocones is demonstrated to have dramatic and broadband absorption enhancement. On the one hand, the metallic core can support plasmonic modes that can provide strong near field enhancement inside the thin semiconductor nanoshell and greatly increase the absorption efficiency of an individual optical mode.[16,21] On the other hand, the nanocone geometry enables the linearly gradient radius of the semiconductor shell, which can generate multiple optical resonances, critical for the broadband absorption enhancement.[7] Because the incident light with different wavelengths can be effectively coupled into the active materials at cross-sectional area of different radius in the core−shell structures, a considerable longer optical path length than the equivalent flat thin film is achieved. This concept ensures much less active material required for sufficient light absorption.

The schematic diagram of the core−shell nanocone structure is shown in Figure 1a. To demonstrate this effect of the design, c-Si, one of the most important PV materials but also a weak absorber, is chosen as the active material.[14] The plasmonic material of the core is chosen as silver (Ag) because of a relatively low intrinsic ohmic loss.[22] For the feasibility of

Received: January 1, 2014
Revised: January 10, 2014
Published: January 20, 2014

   dx.doi.org/10.1021/nl500008y | *Nano Lett.* 2014, 14, 1093−1098

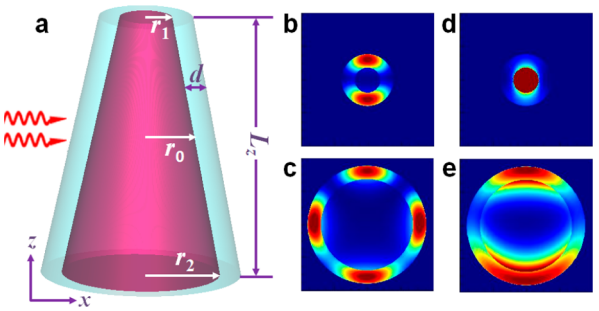

Figure 1. (a) Schematic diagram of a metal-core/semiconductor-shell nanocone, with r_1, r_2, r_0 representing the metallic core radius of the upper, middle, and bottom cross-sectional area, respectively. d is the shell thickness of the semiconductor, and L_z is the axial length of the nanocone. (b,c) Examples of typical absorption mode profiles of (b) 1st order and (c) 2nd order FP modes excited on different wavelengths at different xy-cross-sectional planes: (b) λ = 400 nm, r_0 = 15 nm; (c) λ = 430 nm, r_0 = 55 nm. (d,e) Examples of typical absorption mode profiles of (d) plasmonic and (e) hybrid modes excited on different wavelengths at different xy-cross-sectional planes: (d) λ = 570 nm, r_0 = 15 nm; (e) λ = 520 nm, r_0 = 55 nm.

fabrication processes and simplicity of discussions, the shell thickness of c-Si (noted as d in Figure 1a) is homogeneous along the surface of Ag core. The radius of the middle cross-sectional area of the nanocone is noted as r_0, which is equal to $(r_1 + r_2)/2$ (r_1, r_2 is the radius of the top and bottom cross-sectional area respectively, with $r_1 < r_2$). The length of the nanocone along the z-axis is L_z. In our model, the incident light propagates perpendicular to the axis of the nanocone, and the definition of TM (TE) polarized light is that the **E**-component (**H**-component) is parallel to the z-axis.[23] By solving Maxwell equations with proper boundary conditions, optical modes of infinitely long core−shell cylinder of a definite radius can be calculated. For an infinite Ag-core/c-Si-shell nanowire under perpendicular light illumination, one can steer the optical resonances by tuning the size of the nanowire,[24,25] which can be divided into three types, that is, Fabry−Perot (FP) modes, plasmonic modes, and hybrid modes that combines both the FP and plasmonic features. In a geometrical optics picture, the FP modes here can be regarded as light ray cycling around the nanoshell with totally internal reflection at both the Ag/c-Si and Air/c-Si interfaces. Thus they can be referred to the circular geometrical resonances because of similarity to the standing waves in thin films.[24] In other words, when an FP mode is excited, the EM field is circularly resonant around the metallic core with the maximum EM field inside the semiconductor shell layer. Such a mode can be a TE or TM mode provided that the proper FP resonant condition is fulfilled, which can be noted as TE_{nl} or TM_{nl} respectively (The mode order n is referred to the number of maxima around the resonant circumference while the mode order l referred to the number of maxima in the radius direction).[25,26] Figure 1b (c) shows an example of the typical absorption mode profile of TM_{11} (TM_{21}) of FP mode, which is located in the r_0 = 15 nm (r_0 = 55 nm) 2D cross-sectional area at λ = 400 nm (λ = 430 nm) respectively. As a plasmonic mode is excited, the EM field is greatly confined and exponentially decayed away from the curved metal−semiconductor interface. Such plasmonic modes are mainly related to the LSP resonance and field enhancement is produced in very close proximity to the metal (~10 nm).[18] Thus, in our design the nanoshell thickness d is fixed as 16 nm around which the plasmonic enhancement effect on the absorption of the curved active layer is most effective. Examples

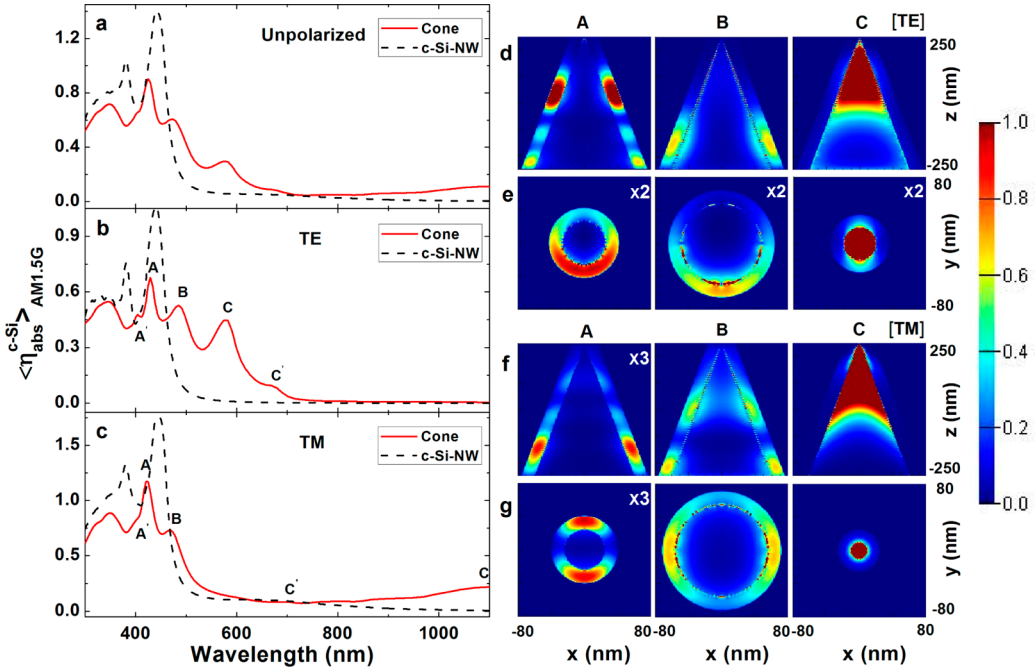

Figure 2. (a−c) The 3D FDTD calculated semiconductor absorption spectra of the proposed nanocone structure (solid line) with geometrical parameters r_1 = 0, r_2 = 60 nm, d = 16 nm, and L_z = 500 nm. Silver and c-Si are employed as the metal core and semiconductor shell materials: (a) unpolarized, (b) TE, and (c) TM illuminations, respectively. The black dashed line represents solid c-Si nanowire with the equivalent mass of c-Si to the core−shell nanocone. (d−g) Normalized absorption mode profiles inside the nanocone for the absorption peaks [from left to right columns are refers to A, B, C noted in panels b and c, respectively]: (d,e) for the TE and (f,g) for the TM illumination; (d,f) for the xz-cross-sectional plane (y = 0) and (e,g) for the corresponding xy-cross-sectional plane with the same transverse core radius as in (d,f) respectively.

dx.doi.org/10.1021/nl500008y | Nano Lett. 2014, 14, 1093−1098

of a typical plasmonic mode profile at r_0 = 15 nm cross-sectional area is shown in Figure 1d, which is excited with a TE polarized light at λ = 570 nm. Besides the FP mode and plasmonic mode, there exists the third type of optical mode, for example, the mode excited at r_0 = 55 nm cross sectional area with a TM polarized light at λ = 520 nm, as is shown in Figure 1e. Because the dependence of the EM field on the radius demonstrates both the FP-like and plasmonic features (see Figure 1e), it is called the hybrid mode. Following the definition of the FP modes, the plasmoinc mode (Figure 1d) and hybrid mode (Figure 1e) are related to TE_{11} and TM_{11} mode, respectively. Note that the nanocone geometry can provide a variety of cross-sectional areas in the 2D core−shell profile, leading to different orders of optical modes in different sizes of core−shell cross-sectional areas. This means that under appropriate design of the metal-core/semiconductor-shell nanocones broadband and significant absorption enhancement can be expected, provided that more optical modes with wavelengths located inside the absorption band of c-Si can be excited in different transverse cross-sectional areas of the structure.

To quantify the absorption performance of the proposed nanocone structure, the definition of the absorption efficiency of the active material c-Si is introduced[24,25]

$$\eta_{\mathrm{abs}}^{\mathrm{c-Si}} = \frac{C_{\mathrm{abs}}}{C_{\mathrm{geo}}} \tag{1}$$

where C_{abs} and C_{geo} are the absorption and geometrical cross sections of the nanocone, respectively. For a single nanocone, C_{abs} is directly determined by the absorption coefficient of the active materials (or imaginary part of the dielectric function ε'') as well as the **E** field intensity distributions inside the c-Si nanoshell layers. C_{geo} is the transverse projected area and can be set as the maximal trapezoid area here.

When averaged over the standard AM1.5G solar spectrum, we can obtain the normalized absorption efficiency $\langle \eta_{\mathrm{abs}}^{\mathrm{c-Si}} \rangle_{\mathrm{AM1.5G}}$ as

$$\langle \eta_{\mathrm{abs}}^{\mathrm{c-Si}} \rangle_{\mathrm{AM1.5G}} = \frac{\int \eta_{\mathrm{abs}}^{\mathrm{c-Si}}(\lambda) F(\lambda)\, \mathrm{d}\lambda}{\int F(\lambda)\, \mathrm{d}\lambda} \tag{2}$$

here $F(\lambda)$ is the photon flux density in the AM1.5G solar spectrum.[27] The integrated waveband region in eq 2 is set from 300 to 1100 nm.

We can also define an integrated short current density (J_{sc}) that is area independent, assuming that all generated electron−hole pairs contribute to the photocurrent

$$J_{\mathrm{sc}} = e \int \frac{\eta_{\mathrm{abs}}^{\mathrm{c-Si}}(\lambda) F(\lambda)}{\frac{hc}{\lambda}}\, \mathrm{d}\lambda \tag{3}$$

The normalized optical absorption efficiency curves of c-Si in a core−shell nanocone for the unpolarized, TE, and TM polarizations are shown in solid lines in Figure 2, which are calculated by eq 2 based on the three-dimensional finite-difference time-domain simulations (3D FDTD, FDTDSolutions @ Lumerical Company, Version 8.6). The absorption curve (solid line shown in Figure 2a) for unpolarized light is obtained by averaging the TE and TM absorption efficiencies. The geometrical parameters of the nanocone are r_1 = 0, r_2 = 60 nm, d = 16 nm and L_z = 500 nm. For clear demonstration, the corresponding absorption curves of the referenced structure, that is, the solid c-Si nanowire (c-Si-NW) with equivalent mass of the active materials, are plotted in Figure 2a−c as well (the black dashed lines). It is observed from the unpolarized absorption curve in Figure 2a that there are more absorption peaks dispersed across 300−1100 nm region compared with that of the equivalent solid c-Si-NW, which leads to the broadband optical absorption enhancement in the visible and near-infrared region. The total effect of the broadband absorption effect of the nanocone structure can be characterized by the enhancement of the integrated efficiency $\langle \eta_{\mathrm{abs}}^{\mathrm{c-Si}} \rangle_{\mathrm{AM1.5G}}$. $\langle \eta_{\mathrm{abs}}^{\mathrm{c-Si}} \rangle_{\mathrm{AM1.5G}}$ of the nanocone structure with only 16 nm thick-shell active materials reaches 25%, which shows about 23% increment compared with that of the equivalent solid c-Si-NW, and is equivalent of the absorption of a 500 nm thick flat c-Si film as well. To further explore the mechanism, the absorption curves of TE and TM polarizations are plotted in Figure 2b,c as well, both of which exhibit multiple-peak profiles (as noted as A (A′), B, C (C′) in Figure 2b,c). For TE illumination, these increased absorption peaks are mainly located around 450−700 nm where the radiation peak of solar spectrum is located. For TM illumination, besides slight broadband absorption near 450−500 nm, there is an extra absorption boost from 800 to 1100 nm (especially near the absorption edge of c-Si). All of these broadband absorption channels greatly compensate the relatively poor performance in the short wavelength region (see Figure 2b,c) and the appealing absorption enhancement under the random polarized solar spectrum can be expected.

To further confirm the underlying mechanism of the broadband absorption enhancement, the normalized absorption mode profiles inside the nanocone of the three typical peaks (A, B, and C) for both TE and TM polarizations have been plotted in Figure 2d−g (profiles from left to right columns are related to A, B, and C respectively). Figure 2d,f shows the subtracted 2D profiles in the *xz*-cross-sectional plane for TE and TM polarizations, while Figure 2e,g shows those in the *xy*-cross-sectional plane. First, an overall landscape can be clearly observed from the *xz*-cross-sectional distributions (Figure 2d,f) that the strong absorption peaks at different wavelengths show field confinement inside the c-Si nanoshell in different transverse cross-sectional core−shells, which are crucial to the broadband absorption effect. It is clear that based on the analysis of these absorption features that these optical modes can be divided into three types, that is, the FP mode, the plasmonic mode and hybrid mode. The absorption peak A (and A′) located in the short wavelength region for both TE and TM polarizations can be ascribed to the FP mode with a typical FP-like resonant profile feature. In addition, the wavelengths of the two modes in both polarizations are in close proximity. It can be ascribed to the mode degeneration of TE_{01} and TM_{11} that have been discussed in the cylinder system before.[24] Such FP modes can greatly increase the optical path length due to the circular resonances, therefore, the absolute absorption efficiency of mode A is relatively higher (compared to the other optical modes such as B and C). The absorption peak C (C′) located in the long wavelength region for both TE and TM polarizations can be ascribed to plasmonic modes, since the field profiles exhibit a pronounced plasmonic feature, that is, the strong near-field enhancement around the curved Ag/c-Si interfaces. The difference is that, the peak C in TE polarization is related to TE_{11} mode, while it is related to TM_{01} mode in TM polarization, as can be observed in the *xy*-cross sectional field profiles, both of which may dominate the absorption in the

dx.doi.org/10.1021/nl500008y | Nano Lett. 2014, 14, 1093−1098

case of ultrasmall core radius (see column III in Figure 2d,f). Because TE_{11} and TM_{01} are not degenerated (located far from each other), peak C (the plasmonic mode) contributes most to the broadband effect in the visible and near-infrared region. Apart from peak A (FP mode) and C (plasmonic mode), there is a third absorption peak (B) in both polarization configurations. Because the field profiles of B (see column II in Figure 2d–g) show both the FP-resonant and plasmonic features, it is categorized as the hybrid mode. The circular resonant feature of FP-mode makes the absolute absorption efficiency of B relatively high, while the plasmonic feature can lead the mode to be slightly red-shifted (compared to the pure FP-like mode), which may broaden the absorption bandwidth (around 500 nm for both polarizations). Finally, it is noted that most field profiles of these absorption peaks are asymmetric, indicating that few of them are pure FP resonances or pure plasmonic resonances or in other words they are the superposition of different types of optical modes. These three types of optical modes compensate with each other across the solar spectrum and contribute significantly to the broadband absorption enhancement.

The optical properties of core–shell nanocones are strongly dependent on the geometric parameters. Figure 3 shows the

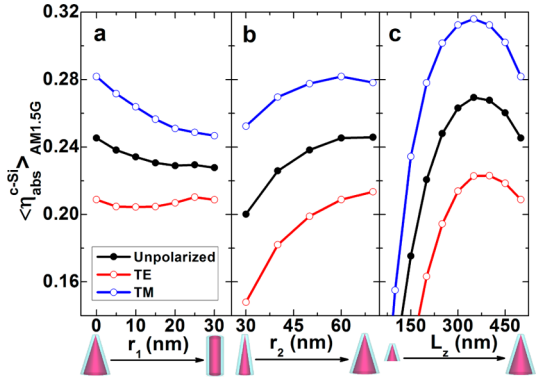

Figure 3. Dependence of the normalized c-Si absorption efficiency $\langle\eta_{abs}^{c\text{-}Si}\rangle_{AM1.5G}$ on (a) upper radius r_1 (with r_0 = 30 nm, d = 16 nm, and L_z = 500 nm fixed), (b) bottom radius r_2 (with r_1 = 0 nm, d = 16 nm, and L_z = 500 nm fixed), and (c) axis length L_z (with r_1 = 0, d = 16 nm, and vertex angle fixed), respectively. The blue (red) hollow-circle line and black solid-circle line represent the TM (TE) and unpolarized illumination, respectively.

dependence of the absorption efficiency of c-Si on the geometrical parameters in three cases. In all the calculations, the thin nanoshell thickness (d = 16 nm) is fixed. In Figure 3a, the middle radius r_0 = 30 nm and the nanocone length L_z = 500 nm are invariant. Thus, the increment of r_1 is accompanied with the simultaneously decrement of r_2, which means that the volume (or mass) of c-Si is unchanged. It is clearly depicted that steeper nanocone structure (with higher radius ratio r_2/r_1) is more efficient for light absorption. Therefore, the core–shell nanowire ($r_1 = r_2$ = 30 nm) is the least absorptive. The physical mechanism can be understood qualitatively as follows. The core–shell nanowire with the same core radius along the axis can only provide the definite optical mode. Although the absorption at the exact wavelength is efficient, the integrated absorption efficiency is quite limited because of the narrow band feature. On the contrary, the steeper nanocone geometry can support more optical modes in the linearly gradient core–shell cross sectional areas, leading to the more broadened absorption band and higher integrated optical absorption. For the steepest nanocone (r_1 = 0 nm) in Figure 3a, the dependence of the absorption efficiency on the bottom radius r_2 is calculated as shown in Figure 3b. With the increment of r_2, the absorption efficiency tends to be saturated, which means that r_2 = 60 nm here is enough for sufficient absorption. In addition, the absorption efficiency also shows the distinct dependence on the nanocone length L_z, as shown in Figure 3c (the vertex angle of the nanocone is fixed as the same as the optimal case in Figure 3a). The appealing feature is that there exists an optimal nanocone length. On the one hand, nanocones with short axis length are less absorptive because relatively less optical modes can be confined. On the other hand, the absorption efficiency of nanocones can not support the linear increment with the axis length, because the absorption band considered here is limited (300–1100 nm) due to the solar spectrum and the selected active material. Or in other words, when the nanocone length exceeds a critical value, the extra length of nanocone can only improve the C_{geo} (the denominator in eq 1) but contribute little to the optical modes and light absorption. Therefore, it is not surprising that there is an optimal length for the angle-fixed nanocone. Here in Figure 3, the maximal absorption efficiency of the optimized nanocone with geometry parameters r_1 = 0, r_2 = 42 nm, L_z = 350 nm, and d = 16 nm reaches up to 27% (nanocones with larger angles can obtain an even larger optimized absorption), which suggests that such core–shell nanocone structures might be ideal building blocks for solar devices.

Finally, taking the optimized nanocone design in Figure 3 for example, we have plotted the spectral short current density $J_{sc}(\lambda)$, as shown in Figure 4. Compared with the referenced

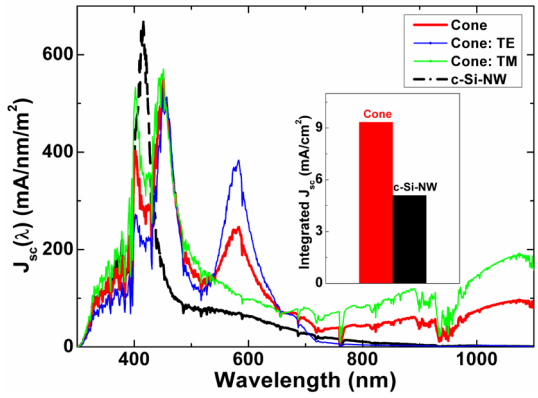

Figure 4. Spectral short-circuit current density for the optimized nanocone solar cell in Figure 3 with r_1 = 0, r_2 = 42 nm, d = 16 nm, and L_z = 350 nm: the unpolarized (red thick solid line), TE-polarized (blue thin solid line) and TM-polarized (green thin solid line) standard solar illumination of AM1.5G, respectively. $J_{sc}(\lambda)$ of the solid c-Si-NW with the equivalent c-Si mass is depicted in black dashed line as the reference. The inset is the integrated J_{sc} for nanocone (red) and c-Si-NW (black), respectively.

solid c-Si-NW, $J_{sc}(\lambda)$ of the optimized nanocone is greatly broadened in the visible and near-infrared region. The effect of the plasmonic-like absorption enhancement (for the TM polarization) from 700 to 1100 nm as well as both hybrid and plasmonic-like broadband absorption from 450 to 650 nm (the radiation region of the solar spectrum peak) can be clearly observed in the $J_{sc}(\lambda)$ spectrum. The integrated J_{sc} of such nanocone is about 9.33 mA/cm^2, which is nearly 183% of the

dx.doi.org/10.1021/nl500008y | Nano Lett. 2014, 14, 1093–1098

solid c-Si-NW (with the same mass of c-Si) and equivalent to a 700 nm thick flat thin film of c-Si. This means that the absorption enhancement factor of the design approaches to the Yablonovitch limit.[11] With proper design and optimization, the nanophotonic structures can provide even higher absorption enhancement that may go beyond this conventional limit.[28]

So far, we have demonstrated a novel design, metal-core/semiconductor-shell nanocones with significant and broadband solar absorption enhancement. The unique nanocone geometry can support broadband circularly resonant optical modes, and the excitations of three types of optical modes contribute to the strong absorption enhancement in the visible and near-infrared region. Detailed parameter optimizations reveal that the steeper nanocones with relatively small metallic cores are favorable for improving energy conversion efficiency. The two key components of the design are the metallic nanocones and the conformal semiconductor shells. There are several well-known semiconductor deposition tools for the conformal thin film coating, such as chemical vapor deposition (CVD), atomic layer deposition (ALD).[29] Also a variety of metallic,[30] semiconductor,[7,31,32] core−shell[8] nanocones have been experimentally fabricated combining both top-down and bottom-up approaches. Those experiments may shed light on the fabrication of the proposed core−shell metal/semiconductor nanocones. Therefore, such a design can be applied to a variety of semiconductors, especially those with relatively low absorption coefficient, and hold promise for the low-cost, high-efficiency solar conversion and water-splitting devices.

AUTHOR INFORMATION

Corresponding Author

*E-mail: jiazhu@nju.edu.cn.

Notes

The authors declare no competing financial interest.

ACKNOWLEDGMENTS

This work is jointly supported by the National Natural Science Foundation of China (NSFC Nos. 11321063 and 11204139) and the Priority Academic Program Development of Jiangsu Higher Education Institutions (PAPD). Partial support is also provided by the University Science Foundation (No. 13KJD140001) and Qing Lan Project of Jiangsu Province.

REFERENCES

(1) Tian, B.; Zheng, X.; Kempa, T. J.; Fang, Y.; Yu, N.; Yu, G.; Huang, J.; Lieber, C. M. Coaxial silicon nanowires as solar cells and nanoelectronic power sources. *Nature* **2007**, *449*, 885−889.

(2) Garnett, E.; Yang, P. D. Light Trapping in Silicon Nanowire Solar Cells. *Nano Lett.* **2010**, *10*, 1082−1087.

(3) Garnett, E. C.; Brongersma, M. L.; Cui, Y.; McGehee, M. D. Nanowire Solar Cells. *Annu. Rev. Mater. Sci.* **2011**, *41*, 269−295.

(4) Hu, L.; Chen, G. Analysis of Optical Absorption in Silicon Nanowire Arrays for Photovoltaic Applications. *Nano Lett.* **2007**, *7*, 3249−3252.

(5) Kelzenberg, M. D.; Turner-Evans, D. B.; Kayes, B. M.; Filler, M. A.; Putnam, M. C.; Lewis, N. S.; Atwater, H. A. Photovoltaic Measurements in Single-Nanowire Silicon Solar Cells. *Nano Lett.* **2008**, *8*, 710−714.

(6) Fan, Z. Y.; Razavi, H.; Do, J. W.; Moriwaki, A.; Ergen, O.; Chueh, Y. L.; Leu, P. W.; Ho, J. C.; Takahashi, T.; Reichertz, L. A.; Neale, S.; Yu, K.; Wu, M.; Ager, J. W.; Javey, A. Three-dimensional nanopillar-array photovoltaics on low-cost and flexible substrates. *Nat. Mater.* **2009**, *8*, 648−653.

(7) Zhu, J.; Yu, Z.; Burkhard, G. F.; Hsu, C.; Connor, S. T.; Xu, Y.; Wang, Q.; McGehee, M.; Fan, S.; Cui, Y. Optical Absorption Enhancement in Amorphous Silicon Nanowire and Nanocone Arrays. *Nano Lett.* **2009**, *9*, 279−282.

(8) Jeong, S.; Garnett, E. C.; Wang, S.; Yu, Z. F.; Fan, S. H.; Brongersma, M. L.; McGehee, M. D.; Cui, Y. Hybrid Silicon Nanocone-Polymer Solar Cells. *Nano Lett.* **2012**, *12*, 2971−2976.

(9) Wei, W. R.; Tsai, M. L.; Ho, S. T.; Tai, S. H.; Ho, C. R.; Tsai, S. H.; Liu, C. W.; Chung, R. J.; He, J. H. Above-11%-Efficiency Organic-Inorganic Hybrid Solar Cells with Omnidirectional Harvesting Characteristics by Employing Hierarchical Photon-Trapping Structures. *Nano Lett.* **2013**, *13*, 3658−3663.

(10) Deceglie, M. G.; Ferry, V. E.; Alivisatos, A. P.; Atwater, H. A. Design of Nanostructured Solar Cells Using Coupled Optical and Electrical Modeling. *Nano Lett.* **2012**, *12*, 2894−2900.

(11) Yablonovitch, E. Statistical ray optics. *J. Opt. Soc. Am.* **1982**, *72*, 899−907.

(12) Kim, S. K.; Day, R. W.; Cahoon, J. F.; Kempa, T. J.; Song, K. D.; Park, H. G.; Lieber, C. M. Tuning Light Absorption in Core/Shell Silicon Nanowire Photovoltaic Devices through Morphological Design. *Nano Lett.* **2012**, *12*, 4971.

(13) Fan, Z. Y.; Kapadia, R.; Leu, P. W.; Zhang, X. B.; Chueh, Y. L.; Takei, K.; Yu, K.; Jamshidi, A.; Rathore, A. A.; Ruebusch, D. J.; Wu, M.; Javey, A. Ordered Arrays of Dual-Diameter Nanopillars for Maximized Optical Absorption. *Nano Lett.* **2010**, *10*, 3823−3827.

(14) Yao, Y.; Yao, J.; Narasimhan, V. K.; Ruan, Z. C.; Xie, C.; Fan, S. H.; Cui, Y. Broadband light management using low-Q whispering gallery modes in spherical nanoshells. *Nat. Commun.* **2012**, *3*, 664.

(15) Li, X. H.; Choy, W. C. H.; Lu, H. F.; Sha, Wei E. I.; Ho, A. H. P. Efficiency Enhancement of Organic Solar Cells by Using Shape-Dependent Broadband Plasmonic Absorption in Metallic Nanoparticles. *Adv. Funct. Mater.* **2013**, *23*, 2728−2735.

(16) Pala, R. A.; White, J.; Barnard, E.; Liu, J.; Brongersma, M. L. Design of plasmonic thin-film solar cells with broadband absorption enhancements. *Adv. Mater.* **2009**, *21*, 3504−3509.

(17) Ferry, V. E.; Munday, J. N.; Atwater, H. A. Design considerations for plasmonic photovoltaics. *Adv. Mater.* **2010**, *22*, 4794−4808.

(18) Ding, I. K.; Zhu, J.; Cai, W. S.; Moon, S. J.; Cai, N.; Wang, P.; Zakeeruddin, S. M.; Cratzel, M.; Brongersma, M. L.; Cui, Y.; McGehee, M. D. Plasmonic dye-sensitized solar cells. *Adv. Energy Mater.* **2011**, *1*, 52−57.

(19) Pillai, S.; Catchpole, K. R.; Trupke, T.; Green, M. A. Surface plasmon enhanced silicon solar cells. *J. Appl. Phys.* **2007**, *101*, 093105.

(20) Schaadt, D. M.; Feng, B.; Yu, E. T. Enhanced semiconductor optical absorption via surface plasmon excitation in metal nanoparticles. *Appl. Phys. Lett.* **2005**, *86*, 063106.

(21) Brittman, S.; Gao, H. W.; Garnett, E. C.; Yang, P. D. Absorption of Light in a Single-Nanowire Silicon Solar Cell Decorated with an Octahedral Silver Nanocrystal. *Nano Lett.* **2011**, *11*, 5189−5195.

(22) Palik, E. D. *Handbook of Optical Constants of Solids*; Academic: New York, 1985.

(23) Cao, L. Y.; White, J. S.; Park, J. S.; Schuller, J. A.; Clemens, B. M.; Brongersma, M. L. Engineering Light Absorption in Semiconductor Nanowire Devices. *Nat. Mater.* **2009**, *8*, 643−647.

(24) Mann, S. A.; Garnett, E. C. Extreme Light Absorption in Thin Semiconductor Films Wrapped around Metal Nanowires. *Nano Lett.* **2013**, *13*, 3173−3178.

(25) Yu, Y.; Ferry, V. E.; Alivisatos, A. P.; Cao, L. Dielectric core-shell optical antennas for strong solar absorption enhancement. *Nano Lett.* **2012**, *12*, 3674−3681.

(26) Coenen, T.; Groep, J.; Polman, A. Resonant modes of single silicon nanocavities excited by electron irradiation. *ACS Nano* **2013**, *7*, 1689−1698.

(27) ASTM G173-03. *Terrestrial Reference Spectra for Photovoltaic Performance Evaluation*; American Society for Testing and Materials: West Conshohocken, PA, 2012.

(28) Yu, Z. F.; Raman, A.; Fan, S. H. Fundamental limit of nanophotonic light trapping in solar cells. *Proc. Natl. Acad. Sci. U.S.A.* **2010**, *107*, 17491−17496.
(29) May, G. S.; Spanos, C. J. *Fundamentals of Semiconductor Manufacturing and Process Control*; John Wiley & Sons: New York, 2006.
(30) Angelis, F. D.; Malerba, M.; Patrini, M.; Miele, E.; Das, G.; Toma, A.; Zaccaria, R. P.; Fabrizio, E. D. 3D Hollow Nanostructures as Building Blocks for Multifunctional Plasmonics. *Nano Lett.* **2013**, *13*, 3553−3558.
(31) Hsu, C. M.; Connor, S. T.; Tang, M. X.; Cui, Y. Wafer-scale silicon nanopillars and nanocones by Langmuir-Blodgett assembly and etching. *Appl. Phys. Lett.* **2008**, *93*, 133109.
(32) Hsu, C. M.; Battaglia, C.; Pahud, C.; Ruan, Z. C.; Haug, F. J.; Fan, S. H.; Ballif, C.; Cui, Y. High-efficiency amorphous silicon solar cell on a periodic nanocone back reflector. *Adv. Eng. Mater.* **2012**, *2*, 628−633.